Article presented at 1st Int Conf Med Sci of North Technical University /Kirkuk, Iraq (1st ICMS 2023)

Original Article

# Extracellular Biosynthesis and Characterization of Silver and Zinc Oxide Nanoparticles Using *Pseudomonas aeruginosa* and *Escherichia coli*

**Baidaa Hamad Attiah, Hiro Mohammed Obaid[1], Siham Shakoor AL-Salihi[1]**

Ministry of Health, Kirkuk Health Department, Al-Mansour Health Center, Kirkuk, [1]Northern Technical University, College of Health and Medical Techniques Kirkuk, Medical Laboratory Techniques Department, Kirkuk, Iraq

Downloaded from http://journals.lww.com/mjby by BhDMf5ePHKav1zEoum1tQfN4a+kJLhEZgbsIHo4XMi0hCywCX1AWnYQp/IlQrHD3i3D0OdRyi7TvSFl4Cf3VC1y0abggQZXdgGj2MwlZLeI= on 04/08/2024

## Abstract

**Background:** The development of dependable and environmentally friendly nanomaterial resources is an essential aspect of recent nanotechnology research and application. Microorganisms have recently been investigated as a potential biofactor for the synthesis of many nanoparticles (NPs). **Objectives:** The aim of this article is to evaluate the extracellular biosynthesis capabilities of metallic NPs such as silver (Ag) and zinc oxide (ZnO) by screening common bacteria. **Materials and Methods:** Silver nitrate and zinc nitrate were used as a source of Ag and ZnO NPs, by means of *Escherichia coli* and *Pseudomonas aeruginosa* as potential candidates for the rapid synthesis of NPs. Ag and ZnO NPs were synthesized using a reduction of aqueous solutions with cell-free filtrates of bacteria. Characterization of synthesized NPs was conducted by UV–Vis spectroscopy. **Results:** Transmission electron microscopy (TEM) was used to examine the particle size of (Ag, ZnO) NPs. The maximum absorbance was around (425, 450 nm) for Ag and (300, 380 nm) for ZnO by *E. coli* and *P. aeruginosa*, respectively. We found that particle size of Ag NP obtained from *P. aeruginosa* was smaller than that of NP obtained from *E. coli*. The range of particle size was 24–32 nm with an average of 29.5 nm for Ag *P. aeruginosa* and was 25–37 nm with an average of 32 nm for Ag *E. coli.* The particle size range of ZnO of *P. aeruginosa* was 23–28 nm with an average of 25 nm and was 25–34 nm with an average of 29.7 nm for *E. coli*. **Conclusion:** *E. coli* and *P. aeruginosa* are good candidates for biosynthesis of NPs. As a result, obliged characteristics and green synthesis and the potential issue for various environmental and health-related applications may exist.

**Keywords:** Biosynthesis, *Escherichia coli*, extracellular, nanoparticle, *Pseudomonas aeruginosa*

## Introduction

Nanotechnology is the process of developing useful technologies and materials at the atomic scale, 100,000 times tinier than a strand of human hair. The abbreviation for nanotechnology is "NANO," which is derived from the Greek word for "dwarf."[1] Top-down and bottom-up approaches are commonly used to create nanoparticles (NPs). The bottom-up approach entails constructing nano structures from either the ground up, atom by atom or molecule by molecule, using nano scale materials (1–100 nm). Microbial cells' production of nano-sized materials has lately become a practical method for the fabrication of metal NPs. NPs are generally classified based on their morphology, dimensionality (D) uniformity, and agglomeration. In 2007, a new nanomaterial (NM) classification scheme was published, which included different residential composites according to the following dimensions: (D) 0D, 1D, 2D, and 3D nano composites.[2] Various biological entities such as bacteria, fungi, algae, yeast, and plants can synthesize a broad range of NPs. Biological reducing agents such as polysaccharides, proteins, enzymes, or microbial metabolites consider an important

Access this article online

Quick Response Code:

Website: https://journals.lww.com/mjby

DOI: 10.4103/MJBL.MJBL_172_22

**Address for correspondence:** Mrs. Baidaa Hamad Attiah, Ministry of Health, Kirkuk Health Department, Al-Mansour Health Center, Kirkuk, Iraq.
E-mail: baidaaatiah@ntu.edu.iq

**Submission:** 14-Aug-2022 **Accepted:** 31-Augt-2022 **Published:** 29-Mar-2024

This is an open access journal, and articles are distributed under the terms of the Creative Commons Attribution-NonCommercial-ShareAlike 4.0 License, which allows others to remix, tweak, and build upon the work non-commercially, as long as appropriate credit is given and the new creations are licensed under the identical terms.

**For reprints contact:** WKHLRPMedknow_reprints@wolterskluwer.com

**How to cite this article:** Attiah BH, Obaid HM, AL-Salihi SS. Extracellular biosynthesis and characterization of silver and zinc oxide nanoparticles using *Pseudomonas aeruginosa* and *Escherichia coli.* Med J Babylon 2023;20:S141-8.

Downloaded from http://journals.lww.com/mjby by BhDMf5ePHKav1zEoum1tQfN4a+kJLhEZgbsIHo4XMi0hCywCX1AWnYQp/IlQrHD3i3D0OdRyi7TvSFl4Cf3VC1y0abggQZXdgGj2MwlZLeI= on 04/08/2024

compound in reducing atoms or ions. Metal NP synthesis in bacteria can occur either intracellularly or extracellularly. Among the various microbes, bacteria have a remarkable ability to reduce heavy metal ions, making them one of the right choices for NP synthesis. The use of *Escherichia coli* for biosynthesis of Ag NPs in an alkaline medium proved that several factors such as pH, temperature, and time affect the size and structure of synthesized NPs.[3] Another researcher has slightly modified the steps by incubating the solution in dark to avoid any photochemical reactions during the experiment.[1] The reported study demonstrates the bacterial isolate of *Pseudomonas aeruginosa* has a good ability for ZnO biosynthesis by using zinc sulfate with cell-free filtrate and 24-h incubation period, a white precipitate formation in the bottom of the flask refers to ZnO NPs.[4] NPs have been fabricated using culture supernatant, aqueous cell-free extract, or bacterial biomass.[5] In order to raise the viability of medicine against multiple germs, green modification of metals and metal oxide can be used as promoters instead of drugs as bacterial resistance to various drug kinds increases. The current study's objective was to isolate *E. coli* and *P. aeruginosa* bacteria and to examine their capacity to produce Ag and ZnO NPs extracellularly.

## Materials and Methods

### Sample collection

The samples collected include wound, burns, and urine from patients who are admitted to the Departments of Azadi Teaching Hospital and Kirkuk General Hospital in order to isolate *P. aeruginosa* and *E. coli*, which is the goal of the current study to biofabricate Ag and ZnO NPs.

### Bacterial isolation

The bacterial isolates of *E. coli* were obtained from bacterial cultures on MacConkey agar. The plates were first inoculated with the bacteria and incubated overnight at 37°C and then single colony cultivated again on blood agar to demonstrate β-hemolysis strain and eosin methylene blue to confirm the bacterial identification.[6] For identification and characterization of the cultured bacteria, the morphological (colony color, shape, and size) and biochemical tests were relied upon. The isolates were characterized as facultative anaerobic, motile, Gram-negative bacteria and showed positive results for catalase test, indole production, and methyl red. Also the strain showed negative result for hydrogen sulfide on triple sugar iron (A/A) due to the bacterium consumption of sucrose and lactose, oxidase test, Voges–Proskauer test, urea hydrolysis, and growth on Simmons Citrate agar slant, as shown in Figure 1. The collected samples of *P. aeruginosa* was inoculated on MacConkey blood agar and incubated for 24 h at 37°C. The isolates' shape, size, color, odor, pigments, and hemolytic activity were all evaluated. After that, a single colony was relocated and streaked on cetrimide agar (a selective medium for isolation of *P. aeruginosa*). All plates were incubated at 37°C for 24 h before transferring a single pure colony to brain heart infusion broth for preservation, and some other biochemical tests that proved the identification of bacteria GN-ID cards were used to confirm the recognized isolates using the automated VITEK-2 compact system. This software analyzes an organism using a methodology based on data characteristics and knowledge about the organism and reaction under investigation.[7]

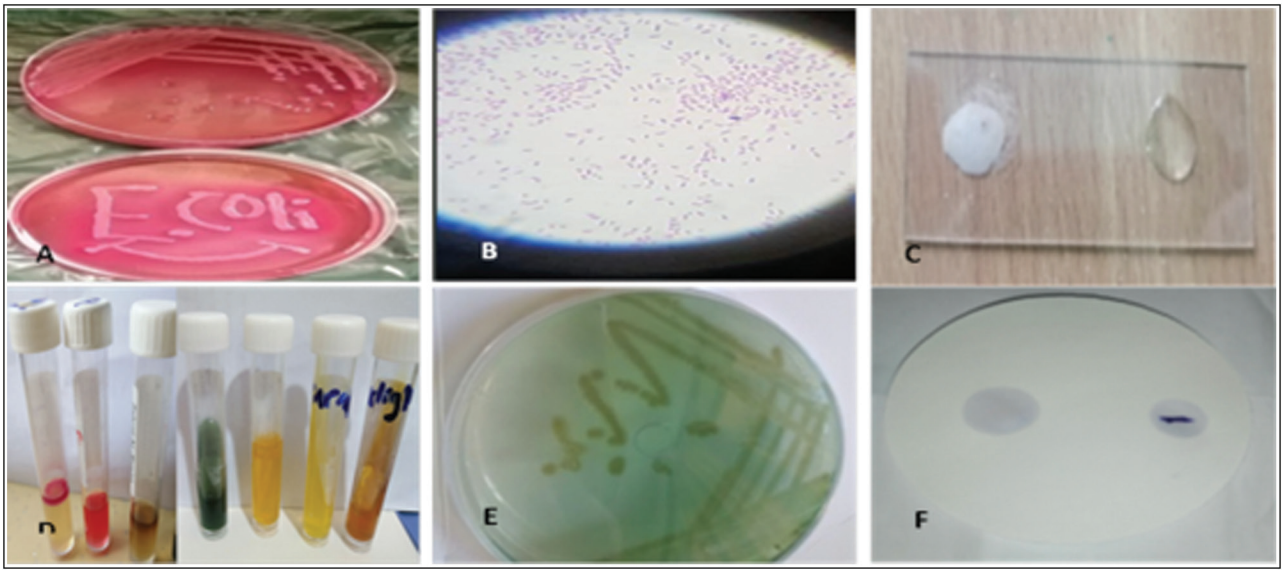


**Figure 1:** Identification tests. (a) *E. coli* culture on MacConkey agar, (b) Gram stain for determining *E. coli* and *P. aeruginosa*, (c) catalase test positive for both bacteria, (d) biochemical test (indole, methyl red, Voges–Proskauer, Simmons Citrate, semi-solid mannitol, urea hydrolysis, TSI tests), (e) *Pseudomonas* pigment on cetrimide agar, (f) oxidase test

Downloaded from http://journals.lww.com/mjby by BhDMf5ePHKav1zEoum1tQfN4a+kJLhEZgbsIHo4XMi0hCywCX1AWnYQp/IlQrHD3i3D0OdRyi7TvSFl4Cf3VC1y0abggQZXdgGj2MwlZLeI= on 04/08/2024

## Biomass production

Pure bacterial isolates inoculated into a 100 mL sterilized nutrient broth container for *P. aeruginosa* and Luria Bertani broth media for *E. coli*, under sterile conditions and incubated at 37°C for 48 h for both bacteria in order to obtain biomass production. After the incubation period, the bacterial cultures were centrifuged at 6000 rpm for 30 min and then cell supernatants were collected for each isolate separately in a sterile flask to use for biosynthesis.[8,9]

## Biosynthesis of nanoparticle

For biosynthesis of silver NPs, 10 mL of bacterial culture supernatant was mixed with 90 mL of 1 mM silver nitrate ($AgNO_3$) solution; another bacterial culture without silver nitrate was used, and silver nitrate solution was used alone as controls to follow the color change. The prepared solutions were incubated at 37°C for 24 h. To avoid any photochemical reaction during the experiment, all solutions were kept in a dark place. After 24 h, the solution changed from yellow to brown indicating the reduction of Ag ions to Ag atom in the presence of aqueous enzymatic extracts in the supernatant solution of bacterial culture. The Ag NPs were purified twice by centrifugation at 10,000 rpm for 5 min and then collected for further analysis.[10] Figure 2(c) illustrates the visual formation of NPs by color change. Biological formation of zinc oxide NPs is obtained by mixing 50 mL of bacterial culture filtrate with 50 mL of zinc nitrate and adjusted the pH of the mixture to 7.0.[11,12] A bacterial mixture with zinc nitrate solution was placed in one of the two flasks: bacterial filtrate was placed in the second and the zinc nitrate solution alone served as the control. At room temperature, cell-free bacterial filtrates were used to reduce an aqueous zinc nitrate solution to create ZnO NPs. In contrast to the control, a white precipitate after 48 h showed the production of ZnO NPs, as shown in Figure 2(d).

## Characterization of nanoparticles

Brown color changing and white precipitate formation were an indication for silver and ZnO NP formation in the reaction mixture, as well as the efficient reduction of Ag ions. To ensure NP formation, the solution absorbance was measured against distinct wave lengths (200–800 nm) by the UV–visible spectrophotometer model (UV-19001J, Shimadzu, Japan); the structural properties of the NPs were characterized by determining the absorbance and verifying that *E. coli* and *P. aeruginosa* extract yielded stable Ag and ZnO NPs. To record and analyze data, the spectrophotometer was outfitted with UV Win Lab software. The spectrophotometer's baseline was corrected using a blank reference. X-ray diffractometer (XRD) measurements were taken at 40 kV and a current of 30 mA with CuK-alpha radiation at a 2° range of 20–80°. For crystal structure of the synthesized NPs, numerical data were plotted in the origin 95 E. To investigate the particle size and lattice image of biosynthesized NPs, a JEOL, Tokyo TEM instrument with an accelerating voltage of 200 kV and a focussed fine beam was used. Samples were prepared by sprinkling one drop of the reaction mixture onto a holey carbon-coated copper TEM grid and allowed to dry in air.[12,13]

### *Ethical approval*

The research was carried out in accordance with the ethical principles outlined in the Helsinki Declaration. Before taking the sample, the patient's verbal and analytical consent was obtained. To obtain this consent, a local ethics committee reviewed and approved the study protocol, subject information, and consent form using the document number 3658 in 11/11/2021.

## Results

One hundred eighty-one samples were collected from different clinical specimens (wound, burn, and urine) and the samples were obtained from patients of different genders and ages (1–60 years), who attended Azadi Teaching Hospital and Kirkuk General Hospital in Kirkuk city, Iraq. In the current study, the most isolated bacteria were *E. coli* 29.3%, and the lowest isolated bacteria was *P. aeruginosa* 24.3%, in contrast to the other

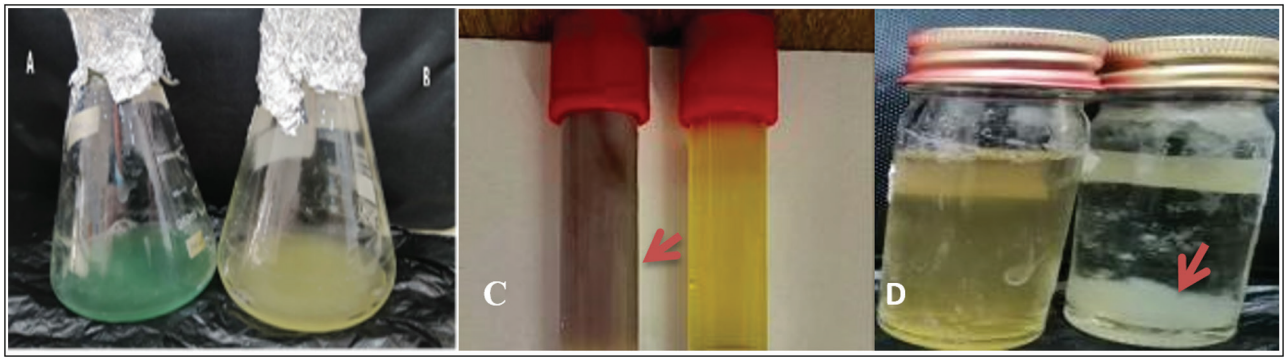


**Figure 2:** Production of biomass: (a) *P. aeruginosa* and (b) *E. coli*. Visual observation of NPs formation: (c) silver production and (d) white precipitates of zinc oxide

Downloaded from http://journals.lww.com/mjby by BhDMf5ePHKav1zEoum1tQfN4a+kJLhEZgbsIHo4XMi0hCywCX1AWnYQp/IlQrHD3i3D0OdRyi7TvSFl4Cf3VC1y0abggQZXdgGj2MwlZLeI= on 04/08/2024

different bacteria isolated (46.4%). The results also noted a significant difference between isolated bacteria species. Tables 1 and 2 illustrate the number, percentage, and distribution of the bacteria.

Cal $\chi^2$= calculated $\chi$, $\chi$ is a value of chi square and was calculated from result data;

Tab $\chi^2$= table $\chi$, $\chi$ is a value of table chi square and calculated from the below law:

$$\text{Degree of freedom} = (\text{No. of columns} - 1) * (\text{No. of rows} - 1)$$

$O_i$ is the observed frequency and $E_i$ is the expected frequency.

*Note*: If calculated $\chi$ is higher than table $\chi$, this indicated a significant difference, whereas if less than table $\chi$, this indicated a non-significant difference.

DF is a degree of freedom and calculated from the below law:

$$\text{Degree of freedom} = (\text{No. of columns} - 1) * (\text{No. of rows} - 1).$$

Pure bacterial isolates were inoculated into a sterilized nutrient broth container for *P. aeruginosa* and Luria-Bertani broth media for *E. coli* under sterile conditions, and the cultures were incubated for 24 h at 30°C for *E. coli* and for 24 h at 37°C for *P. aeruginosa* for biomass production [Figure 2(a) and (b)]. Brown color changing and white precipitate formation were an indication for silver and ZnO NP formation, respectively, in the reaction mixture prepared [Figure 2(c) and (d)].

These changes in the current study demonstrated by UV–visible spectral analysis with spectral range between 200 and 800 nm are shown in Figure 3. The samples exhibited a peak absorption at 425 nm to Ag *E. coli* and at 450 nm to Ag *P. aeruginosa*, whereas the peaks appeared at 300 and 380 nm to ZnO *E. coli*[14] also showed that the exitonic peaks absorption appeared between 300 and 400 nm, which is the typical characteristic of ZnO NP peaks. Absorption of peaks of ZnO was 310 and 378 nm of *P. aeruginosa*, which is near from the previously reported result by AL-Nasrawi and AL-Hashimy[15] who reported that the highest surface plasmon resonance (SPR) was at 380 nm which refers to affluent preformation of metal precursor to final NPs. As shown in Figure 4, XRD plots of Ag *P. aeruginosa* are verified for (111), (200), (220), and (311) planes at $2\Theta$ angles of the diffraction peaks at ~28.08°, 32.48°, 46.48°, and 55.04°. Also similar results were obtained for Ag *E.coli* peaks, reported as ~27.84°, 32.24°, 46.24°, and 54.08° at (111), (200), (220) and (311) planes, respectively.

The XRD ZnO values for *P. aeruginosa* were ~31.85°, 34.55°, 36.35°, and 47.69° for which the corresponding reflections are (100), (002), (101), and (102) planes. The XRD ZnO values for *E. coli* in the listed peak were ~32.04°, 34.72°, 36.56°, and 56.84°, corresponding to (100), (002), (101), and (110) planes.

The results of differences in shapes and size of the synthesized NPs performed by using the TEM image are represented in Figure 5.

**Table 1: Numbers and percentages of the isolated bacteria**

| Bacteria / Gender | *P. aeruginosa* | | *E. coli* | | Other bacteria | | Total | |
|---|---|---|---|---|---|---|---|---|
| | No. | % | No. | % | No. | % | No. | % |
| Male | 15 | 8.3 | 21 | 11.6 | 47 | 26.0 | 83 | 45.9 |
| Female | 29 | 16.0 | 32 | 17.7 | 37 | 20.4 | 98 | 54.1 |
| Total | 44 | 24.3 | 53 | 29.3 | 84 | 46.4 | 181 | 100 |
| Cal $\chi^2$ = 6.731 | | | Tab $\chi^2$ = 5.99 | | DF = 2 | | *P*-value = 0.035 | |

**Table 2: Distribution of samples according to patients' age**

| Bacteria / Age in years | *P. aeruginosa* | | *E. coli* | | Other bacteria | | Total | |
|---|---|---|---|---|---|---|---|---|
| | No. | % | No. | % | No. | % | No. | % |
| < 11 | 5 | 2.8 | 9 | 5.0 | 12 | 6.6 | 26 | 14.4 |
| 11–20 | 8 | 4.4 | 7 | 3.9 | 14 | 7.7 | 29 | 16.0 |
| 21–30 | 7 | 3.9 | 12 | 6.6 | 18 | 9.9 | 37 | 20.4 |
| 31–40 | 11 | 6.1 | 10 | 5.5 | 21 | 11.6 | 42 | 23.2 |
| 41–50 | 7 | 3.9 | 8 | 4.4 | 6 | 3.3 | 21 | 11.6 |
| > 50 | 6 | 3.3 | 7 | 3.9 | 13 | 7.2 | 26 | 14.4 |
| Total | 44 | 24.3 | 53 | 29.3 | 84 | 46.4 | 181 | 100 |
| Cal $\chi^2$ = 4.994 | | | Tab $\chi^2$ = 18.31 | | DF = 10 | | *P*-value = 0.892 | |

Downloaded from http://journals.lww.com/mjby by BhDMf5ePHKav1zEoum1tQfN4a+kJLhEZgbsIHo4XMi0hCywCX1AWnYQp/IlQrHD3i3D0OdRyi7TvSFl4Cf3VC1y0abggQZXdgGj2MwlZLeI= on 04/08/2024

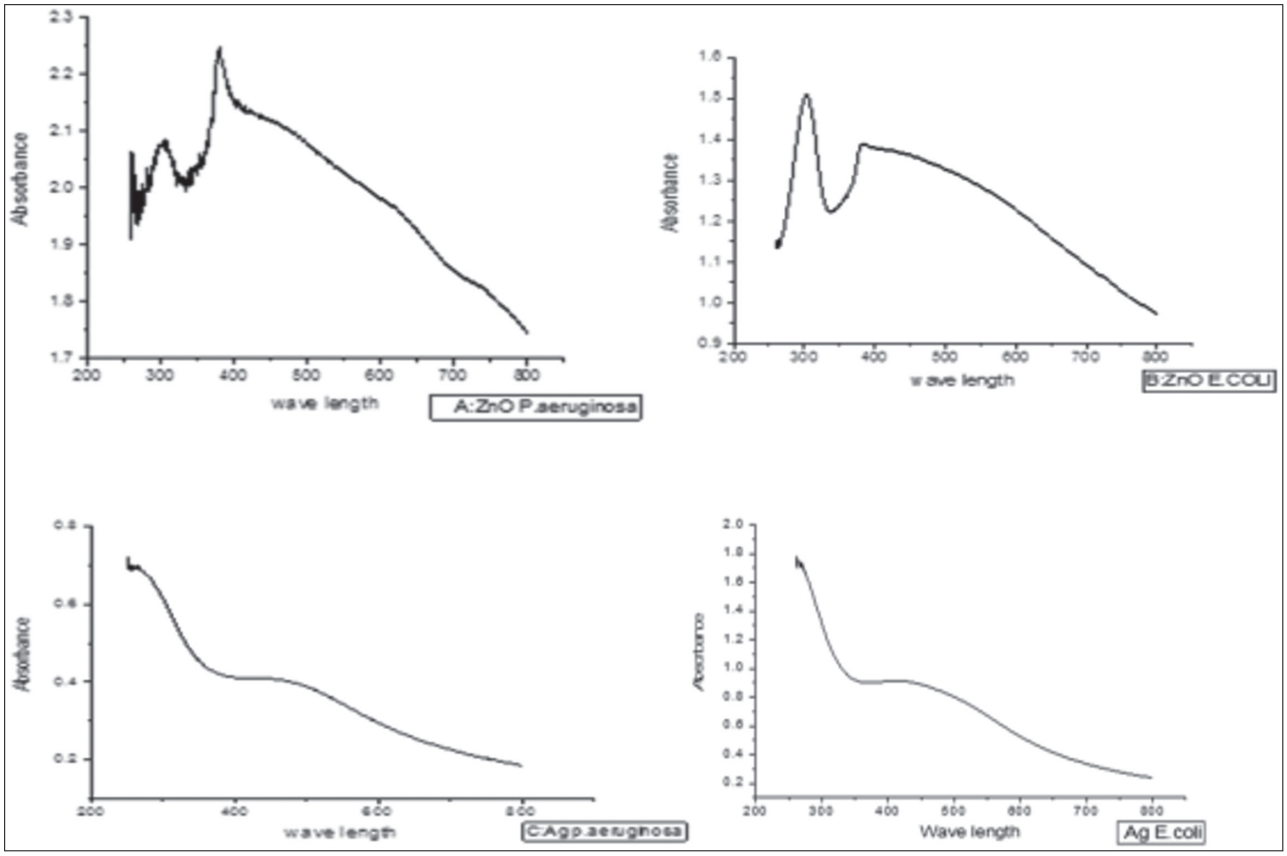


**Figure 3:** UV–visible plots. (a) Absorbance of ZnO *P. aeruginosa*, (b) absorbance of ZnO *E. coli*, (c) absorbance of Ag *P. aeruginosa*, and (d) absorbance of Ag *E. coli*

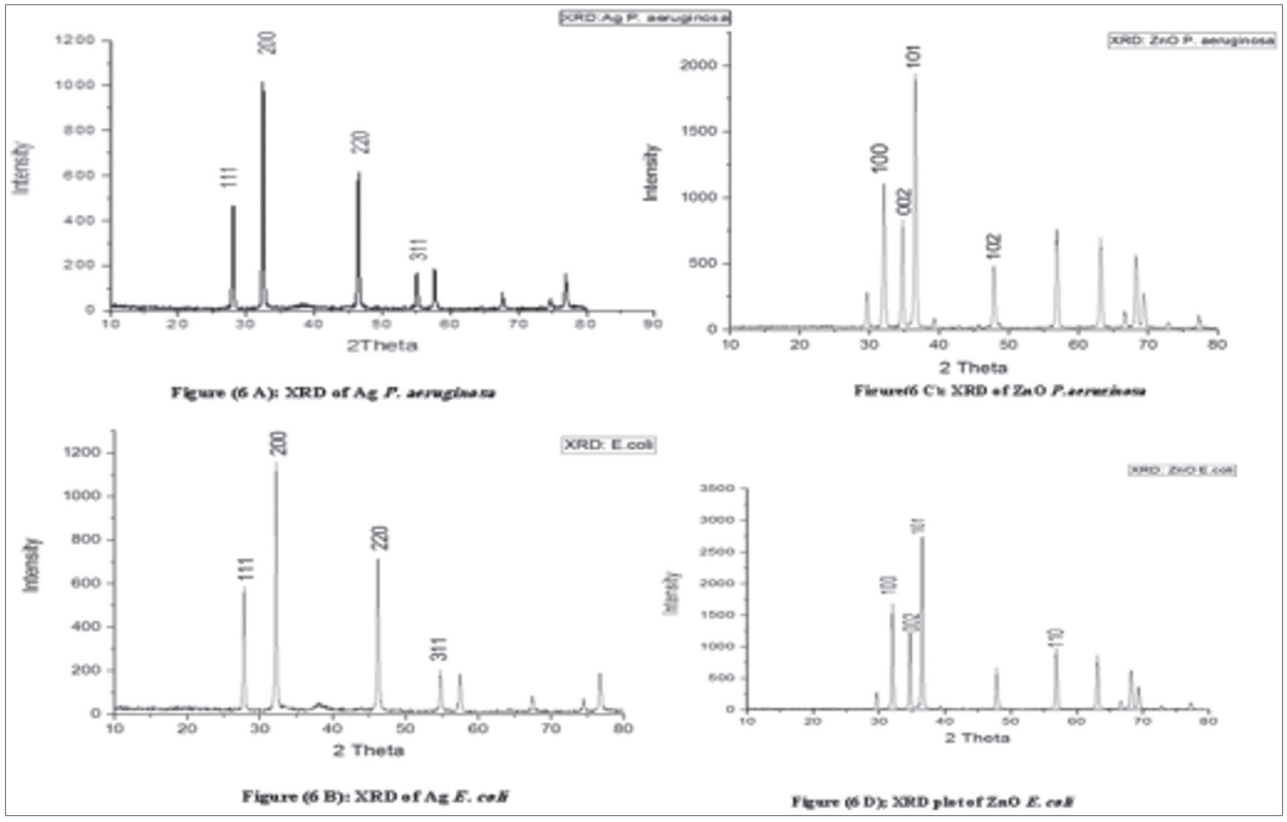


**Figure 4:** XRD plots. (a) XRD Ag *P. aeruginosa*, (b) XRD *E. coli*, (c) XRD ZnO *P. aeruginosa*, and (d) ZnO *E. coli*

Downloaded from http://journals.lww.com/mjby by BhDMf5ePHKav1zEoum1tQfN4a+kJLhEZgbsIHo4XMi0hCywCX1AWnYQp/IlQrHD3i3D0OdRyi7TvSFl4Cf3VC1y0abggQZXdgGj2MwlZLeI= on 04/08/2024

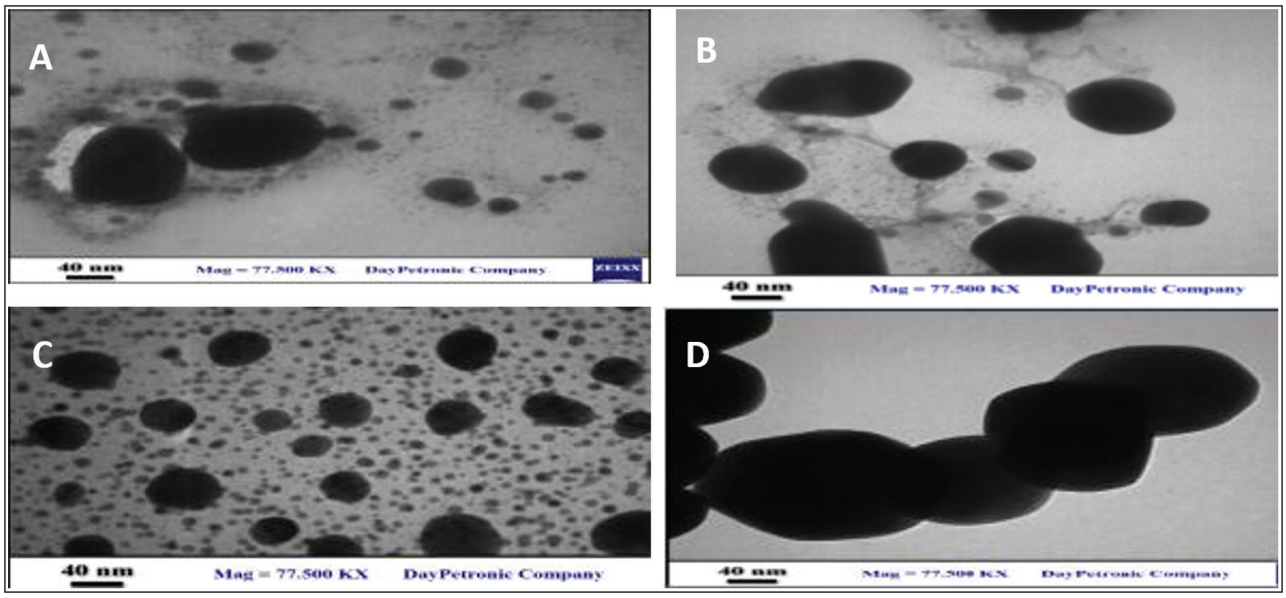


**Figure 5:** TEM images: (a) Ag *E. coli*, (b) Ag *P. aeruginosa*, (c) ZnO *E. coli*, and (d) ZnO *P. aeruginosa*

## Discussion

According to the results, among the 181 collected samples obtained from the statistical analysis, *E. coli* was more prevalent than *P. aeruginosa* at 29.3% and 24.3%, respectively, distributed as 17.7% in females and 11.6% in males, at a *P*-value of less than 0.05. There is a significant difference between the percentage recorded by AL-Nasrawi and AL-Hashimy[15] and the percentage recorded (27.82%) for *E. coli* prevalence among males and females. This is due to the close proximity of the anus to the urethral tube, and female urethral tubes are shorter than male urethral tubes, reducing the distance microorganisms must travel to reach the bladder.[16] Although the *P. aeruginosa* prevalence was 24.3%, this was almost nearly similar to the results of Pandukur *et al*.,[17] who reported that the prevalence of *P. aeruginosa* isolated from wound infections was 26.67%, and to the results of Hasan *et al.*,[18] who reported that the prevalence for *P. aeruginosa* was 21.6%. There was no significant difference among age groups at *P*-value >0.05. The discrepancies in *P. aeruginosa* prevalence between studies could be due to variances in clinical specimens, hospitals, examined populations, geographical areas, and hygienic practices.[18] Also, females had a higher prevalence infection rate for *P. aeruginosa* of 29 (16%) compared with 15 (8.3%) for males at a significant difference of *P*-value=0.035. Non-significant differences between age groups are statistically recorded at *P*-value of 0.892. These results were almost similar to Othman *et al*.[19] who recorded a prevalence of *P. aeruginosa* infection in females more than in males and 27% of isolates were accounted. El Hamzaoui *et al*.[20] determine the prevalence of burn wound infections and report *Pseudomonas* spp. at 18.46% and *E. coli* as the second most common bacteria at 8.46%. The highest level of *E. coli* prevalence in female at 17.7% was recorded by El Hamzaoui *et al*.[20] and Tabassum *et al*.[21] and the lowest level for infection with *E. coli* by Gupta *et al.*[22] was recorded at 6.59%. Following severe burn injuries, sustained hypermetabolism, hormone elevations, and muscle wasting all contribute to the clinical outcomes, with magnitude and duration that are unique to burns.[23] Immunocompromised patients and persons with comorbidities such as diabetes and vascular diseases are mostly susceptible to developing *P. aeruginosa* wound infections, and the severity of the infection depends on the site of infection and on the infecting pathogen.[24]

In this study, we used cell-free culture filtrate of *P. aeruginosa* as a reducing mediator of $AgNO_3$ to form Ag NPs. Initially, the biogenic generation of Ag NPs by *P. aeruginosa* cell-free extract was affirmed visually. The sample exhibited a peak absorption at 425 nm to Ag *E. coli* and at 450 nm to Ag *P. aeruginosa*, which is near to the reported range between 410 and 460 nm from other results.[15,25] The authors reported a strong SPR band ranging from 400 to 550 nm, indicating the formation of Ag NPs.[26] In ZnO, *E. coli* peaks are registered at 300 and 380 nm as in Aldalbahi *et al*.,[14] which showed peaks between 200 and 600 nm. *P. aeruginosa* absorbance of ZnO was at 310 and 378 nm, which is near to previously reported results.[27] The difference in SPR band position was thought to be from bacterial and media components adsorption on the surface of Ag NPs.[28] Extracellular synthesis of Ag NPs by some species of *P. aeruginosa* and *E. coli* is caused by microbial enzyme, proteins, or exopolysaccharides that released in the synthesis media.[26] The natural existence of secondary metabolites such as amino acids, vitamins, and proteins in the biological source prevents the agglomeration of particles during the bio-reduction process.[5,28] Previous reports from TEM

Downloaded from http://journals.lww.com/mjby by BhDMf5ePHKav1zEoum1tQfN4a+kJLhEZgbsIHo4XMi0hCywCX1AWnYQp/IlQrHD3i3D0OdRyi7TvSFl4Cf3VC1y0abggQZXdgGj2MwlZLeI= on 04/08/2024

data disclose that proteins and enzymes stabilize Ag NPs and prevent their accumulation.[29]

For crystal structure of the synthesized Ag NPs, Ag NPs of *P. aeruginosa* clarified that 2$\Theta$ angles of the diffraction peaks were identified at ~28.08°, 32.48°, 46.48°, and 55.04° which are verified for 111, 200, 220, and 311 planes of face-centered cubic (FCC), respectively. They are indexed as cubic phase with lattice constants $a = b$= 6.8830 nm and $c$= 9.1220 nm in a code (202055), which is similar to the results in John *et al.*[30] Moreover, the XRD spectrum showed no peaks other than the characteristic Ag NPs peaks, which confirms that the synthesized NPs were pure. Also, the result of *E. coli* Ag NPs peak is reported as ~27.84°, 32.24°, 46.24°, and 54.08°, which are confirmed with the pattern corresponding to cubic Ag NPs planes of 111, 200, 220, and 311, respectively, with lattice constants $a = b = c$= 4.8160 nm and code 035662. This result is in line with previously reported results.[31,32] This confirms successful synthesis of Ag NPs and establishes their crystalline nature.

The ZnO hexagonal crystal shape reported in code 065119 from the data obtained for *P. aeruginosa* as ~31.85°, 34.55°, 36.35°, and 47.69° corresponds to reflection of 100, 002, 101, and 102 planes which agree with the results of Gunalan *et al*.,[10] who indicate the absence of any impurity and suggest the high purity of synthesized NPs obtained.[33] Furthermore, ZnO NPs obtained from *E. coli* were in a code 065119 in the listed peak, which is nearly similar to Dobrucka and Długaszewska,[34] who concluded that there are good agreements between two patterns, and ZnO NPs were successfully synthesized using this method. The broadening and widening of almost all of the detected peaks could represent very small crystallites on the nanoscale.[34]

The difference in the shapes and sizes of the synthesized NPs was studied using TEM images. Cubic and hexagonal structure with some agglomerated large and small particle is the morphological appearance of synthesized NPs. The size of Ag NPs biosynthesized from *E. coli* at a magnification of 77,500 k× appears roughly cubic which relatively looked uniform in diameter around 32 nm, as reported by another group of investigators[35] who mentioned that the size of Ag NPs is around 25–45 nm. In the recent study, for Ag NPs from *P. aeruginosa* at 27,800 k× magnification power, the size appears at 29.5 nm with different shapes such as rod, hexagonal, and cubic structure. Our results agree with the previously reported results.[30] Most of the ZnO NPs were on the nanometer scale at 25–34 nm for *E. coli* in average (30 nm) and (23–28 nm) for *P. aeruginosa* in average (25 nm) with hexagonal or other various shapes. Surprisingly, the largest amounts of ZnO NPs had the same dimensions as a small amount of large particles. The ZnO NPs also exhibited some agglomeration, which is typical of green NP synthesis. This agglomeration is caused by the fact that green-synthesized NPs have a larger surface area and are highly adherent to one another.[36]

## Conclusion

From the results of the current study, we concluded that both *P. aeruginosa* and *E. coli* bacteria have the ability of biosynthesis of Ag and ZnO extracellularly and that the produced NPs size obtained from *P. aeruginosa* was smaller than those NPs obtained from *E. coli*. ZnO NPs were slightly bigger in size than those obtained from *E. coli*. Hence, we recommend the use extracellular method for NPs production; they are good candidates for producing Ag and ZnO NPs. We also recommend studying the pharmaceutical effect of these NPs on different human and animal pathogens.

### Financial support and sponsorship

Nil.

### Conflicts of interest

There are no conflicts of interest.

## References

1. Kushwaha A, Singh VK, Bhartariya J, Singh P, Yasmeen K. Isolation and identification of *E. coli* bacteria for the synthesis of silver nanoparticles: Characterization of the particles and study of antibacterial activity. Eur J Exp Biol 2015;5:65-70.
2. Pokropivny VV, Skorokhod VV. Classification of nanostructures by dimensionality and concept of surface forms engineering in nanomaterial science. Mater Sci Eng: C 2007;27:990-3.
3. Mahanty A, Bosu RA, Panda P, Netam SP, Sarkar B. Microwave assisted rapid combinatorial synthesis of silver nanoparticles using *E. coli* culture supernatant. Int J Pharm Bio Sci 2013;4:1030-5.
4. Al-jnabi Th YS. Biosynthesis of zinc oxide nanoparticles by *Pseudomonas aeruginosa* locally isolated. University of Baghdad; 2019.
5. Siddiqi KS, Husen A, Rao RAK. A review on biosynthesis of silver nanoparticles and their biocidal properties. J Nanobiotechnol 2018;16:14.
6. Obaid Hiro M, AL-Salihi Siham Sh, Hussein Nuaman F. Human scabies in Kirkuk, Iraq: Prevalence and relation to secondary bacterial infections. Plant Arch 2020;20:9446-52.
7. Nikhil A, Kolte NA, Tumane PM, Wasnik DD. Extracellular biosynthesis and characterization of silver nanoparticles by using *Bacillus cereus* gad 20 and their antibacterial potential against *E. coli* and *S. aureus*. Int J Curr Res 2017;9:61849-56.
8. Kareem DK. Biosynthesis of silver nanoparticles using bacterial cells and determining its effect on some bacterial virulence factors and in inhibiting cancer cells. University of Kirkuk; 2021.
9. Sreeharsha N, Kathiravan G, Rajagopal K, Rajasekar A, Rajangam B, Aldhubiab BE, *et al*. Synthesis, characterization, and biological activity of silver nanoparticles synthesized from *Aristolochia bracteolata* Lam. Pharmacogn Mag 2020;16:568.
10. Gunalan S, Sivaraj R, Rajendran V. Green synthesized ZnO nanoparticles against bacterial and fungal pathogens. Progr Natu Sci Mater Int 2012;22:693-700.
11. Saleh TY. Biosynthesis of zinc oxide nanoparticles by *Pseudomonas aeruginosa* locally isolated. University of Baghdad; 2010.
12. Daphedar AB, Kakkalameli SB, Melappa G, Taranath TC, Srinivasa C, Shivamallu C, *et al*. Genotoxic assay of silver and zinc oxide nanoparticles synthesized by leaf extract of *Garcinia livingstonei* T. Anderson: A comparative study. Pharmacogn Mag 2021;7:114.

Downloaded from http://journals.lww.com/mjby by BhDMf5ePHKav1zEoum1tQfN4a+kJLhEZgbsIHo4XMi0hCywCX1AWnYQp/IlQrHD3i3D0OdRyi7TvSFl4Cf3VC1y0abggQZXdgGj2MwlZLeI= on 04/08/2024


13. Jabir MS, Rashid TM, Nayef UM, Albukhaty S, AlMalki FA, Albaqami J, *et al*. Inhibition of *Staphylococcus aureus* α-hemolysin production using nanocurcumin capped Au@ZnO nanocomposite. Bioinorg Chem Appl 2022;2022:2663812.
14. Aldalbahi A, Alterary S, Ali AR, Awad MA, Aldosari NS, Fahad AS, *et al*. Greener synthesis of zinc oxide nanoparticles: Characterization and multifaceted applications. Molecules 2020;25:4198.
15. AL-Nasrawi MM, AL-Hashimy AB. Molecular study of some virulence genes of *Escherichia coli* isolated from women with urinary tract infection in AL-Najaf city. Iraqi J Biotechnol 2020;3:42-8.
16. Ibrahem EJ. Determine the effectiveness of inhibitory of ZnO and MgO nanoparticles against some species of pathogenic bacteria isolated from patients with urinary tract infections in Sulaymaniya city. Dissertation in University of Tikrit; 2016.
17. Pandukur SG, Sambo TT, Plangnan AG. Prevalence of bacterial pathogens associated with wound infections from diabetic out-patients at Plateau Specialist Hospital, Jos, Nigeria. Open J Niger (OJN) 2020;1:01-11.
18. Hasan SA, Najati AM, Abass KS. Prevalence and antibiotic resistance of "*Pseudomonas aeruginosa*" isolated from clinical samples in Kirkuk City, Iraq. Eurasia J Biosci 2020;14:1821-5.
19. Othman N, Babakir-Mina M, Noori CK, Rashid PY. *Pseudomonas aeruginosa* infection in burn patients in Sulaimaniyah, Iraq: Risk factors and antibiotic resistance rates. J Infect Dev Ctries 2014;8:1498-502.
20. El Hamzaoui N, Barguigua A, Larouz S, Maouloua M. Epidemiology of burn wound bacterial infections at a Meknes Hospital, Morocco. New Microbes New Infect 2020;38:100764.
21. Tabassum N, Akter A, Acharjee M. Prevalence of urinary tract infection among the patients admitted in the Brahmanbaria Medical College Hospital in Bangladesh. Merit Res J Med Sci 2020;8:111-9.
22. Gupta M, Naik AK, Singh SK. Bacteriological profile and antimicrobial resistance patterns of burn wound infections in a tertiary care hospital. Heliyon 2019;5:e02956.
23. Rowan MP, Cancio LC, Elster EA, Burmeister DM, Rose LF, Natesan S, *et al*. Burn wound healing and treatment: Review and advancements. Crit Care 2015;19:243.
24. Raizman R, Little W, Smith AC. Rapid diagnosis of *Pseudomonas aeruginosa* in wounds with point-of-care fluorescence imaging. Diagnostics 2021;11:280.
25. Quinteros MA, Aiassa Martínez IM, Dalmasso PR, Páez PL. Silver nanoparticles: Biosynthesis using an ATCC reference strain of *Pseudomonas aeruginosa* and activity as broad spectrum clinical antibacterial agents. Int J Biomater 2016;2016:5971047.
26. Sable SV, Kawade S, Ranade S, Joshi S. Bioreduction mechanism of silver nanoparticles. Mater Sci Eng C Mater Biol Appl 2020;107:110299.
27. Miri A, Mahdinejad N, Ebrahimy O, Khatami M, Sarani M. Zinc oxide nanoparticles: Biosynthesis, characterization, antifungal and cytotoxic activity. Mater Sci Eng C Mater Biol Appl 2019;104:109981.
28. Zhang XF, Liu ZG, Shen W, Gurunathan S. Silver nanoparticles: Synthesis, characterization, properties, applications, and therapeutic approaches. Int J Mol Sci 2016;17:1534.
29. Sabzevar AH, Hashemitabar GR, Rad M, Vatandoost J. Synthesis and biological properties of silver chloride nanoparticles using cell-free extracts of *Aeromonas hydrophila* and antibacterial activity against drug-resistant bacteria. Braz Arch Biol Technol 2021;19:1-16.
30. John MS, Nagoth JA, Ramasamy KP, Mancini A, Giuli G, Natalello A, *et al*. Synthesis of bioactive silver nanoparticles by a *Pseudomonas* strain associated with the Antarctic psychrophilic protozoon *Euplotes focardii*. Marine Drugs 2020;18:38.
31. Yang J, Wang Q, Wang C, Yang R, Ahmed M, Kumaran S, *et al*. *Pseudomonas aeruginosa* synthesized silver nanoparticles inhibit cell proliferation and induce ROS mediated apoptosis in thyroid cancer cell line (TPC1). Artif Cells Nanomed Biotechnol 2020;48:800-9.
32. Jha AK, Zamani S, Kumar A. Green synthesis and characterization of silver nanoparticles using *Pteris vittata* extract and their therapeutic activities. Biotechnol Appl Biochem 2022;69:1653-62.
33. Singh BN, Rawat AK, Khan W, Naqvi AH, Singh BR. Biosynthesis of stable antioxidant ZnO nanoparticles by *Pseudomonas aeruginosa* rhamnolipids. PLoS One 2014;9:e106937.
34. Dobrucka R, Długaszewska J. Biosynthesis and antibacterial activity of ZnO nanoparticles using *Trifolium pratense* flower extract. Saudi J Biol Sci 2016;23:517-23.
35. Kumar CG, Mamidyala SK. Extracellular synthesis of silver nanoparticles using culture supernatant of *Pseudomonas aeruginosa*. Colloids Surf B Biointerf 2011;84:462-6.
36. Fakhari S, Jamzad M, Kabiri Fard H. Green synthesis of zinc oxide nanoparticles: A comparison. Green Chem Lett Rev 2019;12:19-24.